Stem Cell Reports
Report
OPEN ACCESS

Temporal Control of Retroviral Transgene Expression in Newborn Cells in the Adult Brain

Simon M.G. Braun,[1,2,3] Raquel A.C. Machado,[1,2] and Sebastian Jessberger[1,2,3,*]
[1]Brain Research Institute, Faculty of Medicine, University of Zurich, 8057 Zurich, Switzerland
[2]Institute of Molecular Health Sciences, Department of Biology, Swiss Federal Institute of Technology (ETH) Zurich, 8093 Zurich, Switzerland
[3]Neuroscience Center Zurich, University of Zurich and ETH Zurich, 8057 Zurich, Switzerland
*Correspondence: jessberger@hifo.uzh.ch
http://dx.doi.org/10.1016/j.stemcr.2013.06.003

SUMMARY

Neural stem/progenitor cells (NSPCs) generate new neurons throughout life in distinct areas of the adult mammalian brain. Besides classical transgenesis-based approaches, retrovirus-mediated genetic manipulation is frequently used to study mechanisms that regulate neurogenesis in the nervous system. Here, we show that fusion of a tamoxifen-regulatable estrogen receptor (ER^{T2}) motif to transcription factors (i.e., ASCL1 and NEUROD1) enables temporal control of transgene expression in adult mouse NSPCs in vitro and in vivo. Thus, the approach described here represents a versatile strategy for regulating gene expression to study gene function in dividing cells and their progeny.

INTRODUCTION

Neural stem/progenitor cells (NSPCs) generate new neurons throughout life in distinct areas of the adult mammalian brain, including the subventricular zone (SVZ) lining the lateral ventricles from which newborn cells migrate toward the olfactory bulb and the hippocampal dentate gyrus (DG) (Zhao et al., 2008). Due to the relative sparseness of NSPCs and their progeny in relation to pre-existing neural structures, there is a need to selectively manipulate gene activity in NSPCs and their progeny to address their functional significance during the course of development from a dividing NSPC to a fully mature and synaptically integrated neuron (Dhaliwal and Lagace, 2011).

One approach to test the functional significance of genes/pathways is to use transgenic mice carrying floxed alleles of genes of interest, together with Tamoxifen (TAM)-regulatable Cre-recombinase controlled by NSPC- or immature neuron-selective promoters, to genetically recombine and delete genes (Ihrie et al., 2011; Sahay et al., 2011). In addition, retroviral vectors derived from Moloney murine leukemia viruses have proved to be an important tool to visualize newborn cells through the expression of fluorescent proteins, as well as to manipulate gene expression using both gain- and loss-of-function strategies (Ge et al., 2006; van Praag et al., 2002). The use of retroviruses has the advantage that it is highly selective for dividing cells (i.e., neurogenic cells when injected into the SVZ or DG) and is a very fast method because extensive breeding to obtain correct genotypes, as is the case for classical transgenesis, is not required (Zhao and Gage, 2008).

However, retroviral vectors do not target bona fide NSPCs that are largely quiescent but integrate into highly proliferative neural progenitors, which restrict virus-mediated genetic manipulations to later steps of neurogenesis. Furthermore, current vectors do not allow inducible or temporally controlled expression of the virus-driven transgene. Temporal control of transgene expression would be advantageous for studying gene function during distinct steps in the course of neuronal development. This is especially true for transcription factors (TFs) that may exert stage-specific functions depending on the age of a given newborn cell (Iwano et al., 2012). We reasoned that fusion of a TAM-regulatable estrogen receptor (ER^{T2}) motif (Indra et al., 1999; Jiang et al., 2010) to expression constructs of TFs involved in neurogenesis would enable TAM-induced transgene expression, allowing for temporal control of virus-mediated gene expression (Figures 1A and 1B; Supplemental Experimental Procedures available online).

RESULTS

It was previously shown that *Ascl1* overexpression in cultured adult NSPCs results in robust neuronal differentiation (Jessberger et al., 2008). To analyze whether fusion of *Ascl1* to the ER^{T2} motif leads to functional ASCL1 expression upon TAM treatment, we transduced NSPCs isolated from adult mice with *Ascl1*-ER^{T2}-IRES-GFP (hereafter called *Ascl1*-ER^{T2})-expressing retroviruses in vitro. To induce translocation of the ASCL1-ER^{T2} fusion protein, we treated the cells with hydroxy-TAM (OH-TAM) and analyzed them 7 days after the onset of differentiation. Whereas *Ascl1*-ER^{T2}-expressing cells cultured without OH-TAM did not show any difference in their rate of neuronal differentiation compared with cells transduced with a control

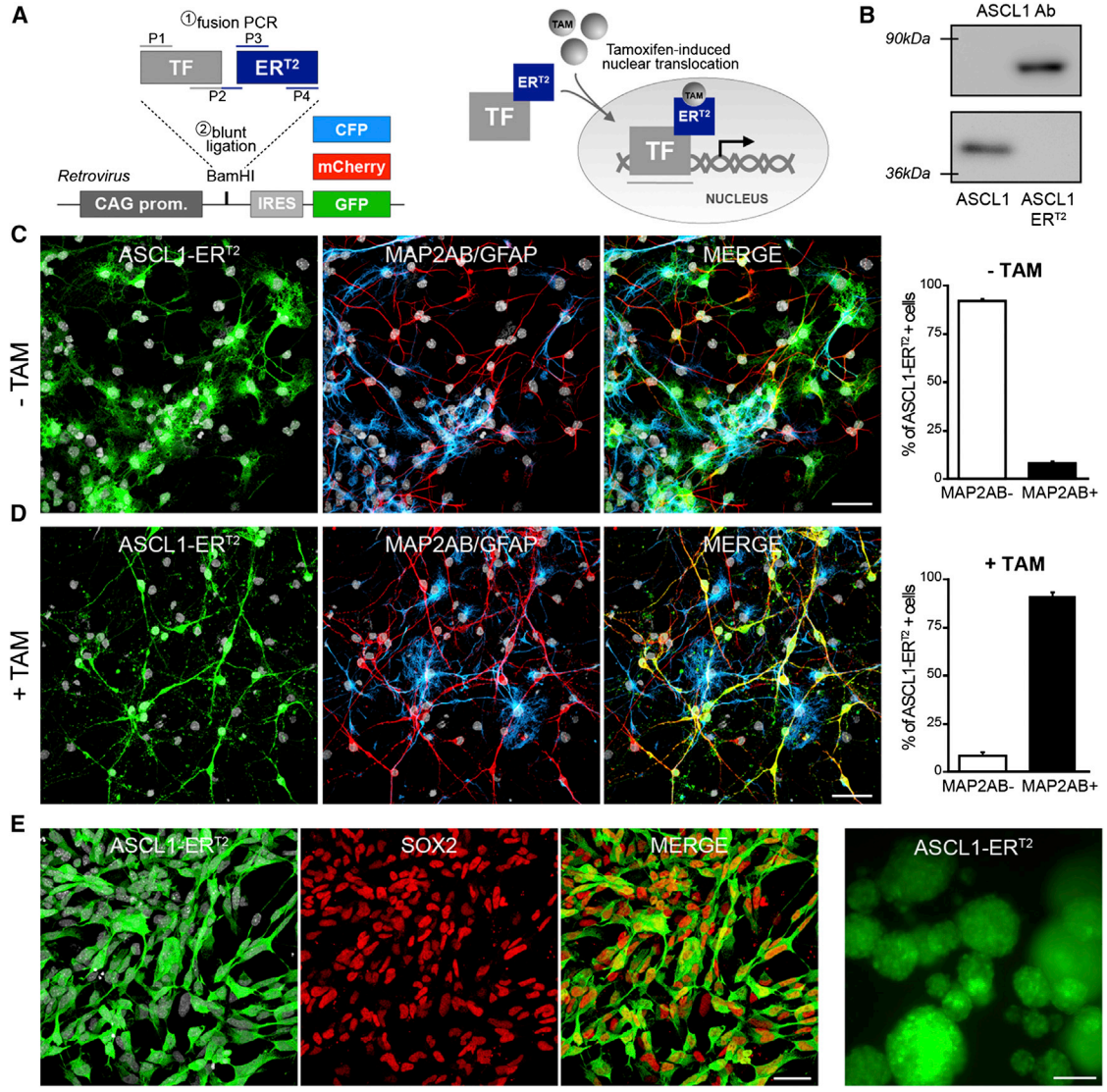

Figure 1. Temporal Control of Retrovirus-Mediated *Ascl1*-ER^{T2} Activity In Vitro

(A) Two-step PCR cloning strategy to fuse an ER^{T2} motif to TFs expressed from a retroviral vector. Upon binding of TAM to the ER^{T2} motif, the TF translocates to the nucleus and regulates target gene transcription.

(B) Western blot analysis reveals the fusion of an ER^{T2} motif to ASCL1, using an ASCL1 antibody to visualize the WT and fusion proteins.

(C) Differentiation of adult NSPCs transduced with *Ascl1*-ER^{T2}-expressing virus (green) without OH-TAM yields only a minority of neuronally differentiated cells expressing MAP2AB (red), whereas most cells differentiate into glial cells expressing GFAP (blue). Right bars show quantifications.

(D) Exposure of *Ascl1*-ER^{T2}-expressing cells (green) to OH-TAM for 4 days leads to the dramatic induction of neuronal differentiation as measured with MAP2AB (red) and a reduction in GFAP-positive cells (blue). Right bars show quantifications. −TAM: 8.04% ± 1.53% neurons; +TAM: 91.58% ± 2.14% neurons; *$p < 0.001$; $n = 3$, biological replicates.

(E) NSPCs transduced with *Ascl1*-ER^{T2}-expressing virus (green) can be properly propagated as monolayers expressing SOX2 (red, left panels) or floating neurospheres in the absence of OH-TAM (right panel), indicating the tight control of virus-mediated gene expression with TAM. Images were taken 10 days after viral transduction.

Error bars represent mean ± SEM. Scale bars represent 40 μm (C, D, and E, left panel) and 100 μm (E, right panel). Nuclei were stained with DAPI (gray).

See also Figures S1 and S3.

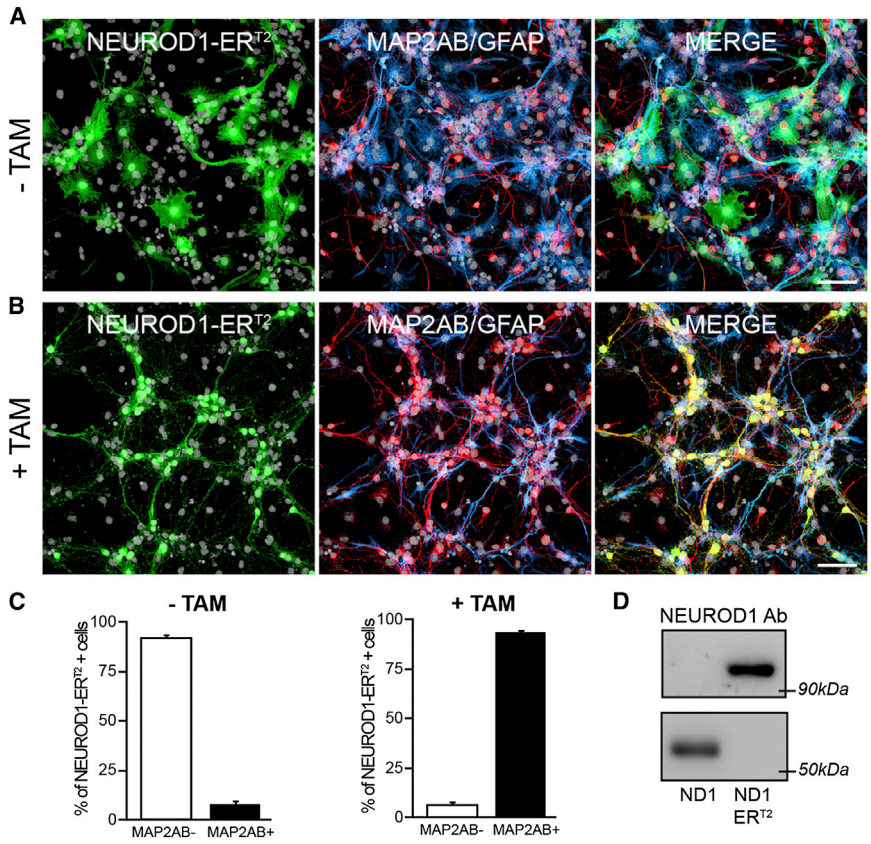

Figure 2. Inducible *NeuroD1* Expression Using TAM in Cultured NSPCs

(A) Differentiation of adult NSPCs transduced with *NeuroD1*-ER^{T2}-expressing virus (green) without OH-TAM does not alter neural differentiation as measured by MAP2AB expression (red) for neuronal cells and GFAP (blue) for glial cells.

(B) Cells transduced with *NeuroD1*-ER^{T2}-expressing virus almost exclusively differentiate into neuronal cells expressing MAP2AB (red) upon OH-TAM exposure.

(C) Quantification of neuronal differentiation of *NeuroD1*-ER^{T2}-expressing cells in vitro with (right graphs) and without OH-TAM exposure (left graphs), indicating the robust control of TAM-regulated gene expression. −TAM: 8.08% ± 1.85% neurons; +TAM: 93.59% ± 1.46% neurons; *$p < 0.001$; $n = 3$, biological replicates.

(D) Western blot analysis reveals the fusion of an ER^{T2} motif to a *NeuroD1* expression construct, using NEUROD1 antibody to visualize the WT and fusion proteins.

Error bars represent mean ± SEM. Scale bars represent 40 μm. Nuclei were stained with DAPI (gray).

See also Figure S2.

retrovirus (expressing IRES-GFP), treatment of *Ascl1*-ER^{T2}-expressing cells with OH-TAM resulted in a dramatic increase in neuronal differentiation (Figures 1C, 1D, S1A, and S1B). These findings suggest that OH-TAM treatment resulted in the robust and efficient transcriptional activation of ASCL1 target genes to induce neuronal differentiation in vitro. To confirm that this approach is applicable to other TFs and not restricted to ASCL1, we fused the basic helix-loop-helix TF NEUROD1 to an ER^{T2} motif (Figure 2D) and infected NSPC cultures with *NeuroD1*-ER^{T2}-IRES-GFP-expressing retroviruses. As before, we observed the almost complete neuronal differentiation of NSPCs upon OH-TAM treatment (Figures 2A–2C). This finding is consistent with the induction of NEUROD1 transcriptional activity, as it was previously shown that NEUROD1 overexpression promotes neuronal differentiation of NSPCs (Gao et al., 2009). Furthermore, we were able to confirm that the subcellular localization of ASCL1-ER^{T2} and NEUROD1-ER^{T2} was indeed controlled by OH-TAM-dependent translocation of the fusion proteins from the cytoplasm to the nucleus of transduced NSPCs (Figures S2A and S2B).

A current limitation in studying neuronal differentiation using cultured NSPCs is that the rate of neuronal differentiation of adult NSPCs is rather incomplete: when standard protocols of growth-factor withdrawal are used, only 8%–30% of NSPC progeny differentiate toward the neuronal lineage (as measured by MAP2AB or TUJ1 expression), whereas the majority of NSPC-derived cells differentiate into glial cells (Babu et al., 2007; Seaberg et al., 2005). Therefore, an inducible system that allows complete and reproducible conversion of undifferentiated NSPCs into neurons would represent a major advantage compared with existing protocols. Thus, we next analyzed whether NSPCs expressing ASCL1-ER^{T2} fusion proteins can be propagated as proliferating neurospheres or monolayer cultures when OH-TAM is absent, and be committed to neuronal differentiation when OH-TAM is added. NSPCs were transduced with *Ascl1*-ER^{T2} expressing retroviruses and cultured for several weeks thereafter. In the absence of OH-TAM, *Ascl1*-ER^{T2}-expressing NSPCs continued to express the NSPC marker SOX2, showed very similar rates of proliferation compared with control cells labeled with a GFP-expressing retrovirus, and could be repeatedly passaged as neurospheres (Figure 1E). Strikingly, the pulse of OH-TAM induced the near-complete differentiation of *Ascl1*-ER^{T2}-expressing NSPCs into neurons (as measured by MAP2AB labeling), indicating that controllable transgene expression is tightly regulated and that transient induction

of *Ascl1* is sufficient to promote neuronal differentiation of cultured NSPCs. Therefore, after an initial induction of ASCL1 transcriptional activity to trigger neuronal differentiation, NSPCs differentiate under normal conditions, as ASCL1-ER^{T2} is no longer active in the absence of OH-TAM. Again, similar results were obtained when we used *NeuroD1*-ER^{T2}-expressing cells, further supporting the feasibility of this inducible approach (data not shown). To analyze the dynamics of *Ascl1*-ER^{T2}-mediated neuronal differentiation in greater detail, we first shortened the time of OH-TAM treatment from 4 days to 2 days, which also resulted in a strong increase in neuronal differentiation (Figures S3A and S3B). In addition, we performed luciferase assays using a basic helix-loop-helix (bHLH) reporter construct as described previously (Castro et al., 2006) to monitor ASCL1 transcriptional activity. We measured a rapid induction of luciferase activity upon OH-TAM treatment (Figure S3C), further confirming the efficacy and tight temporal control of the ER^{T2}-based system.

Next, we sought to analyze whether TAM-inducible *Ascl1*-ER^{T2} gene expression is sufficient to convert NSPC-derived astrocytes toward a neuronal lineage. As shown above, the majority of NSPCs differentiated into glial fibrillary acidic protein (GFAP)-expressing astrocytes after growth-factor withdrawal (Figure 1C). To test whether these astroglia could be converted toward a neuronal fate (Heinrich et al., 2010) using the *Ascl1*-ER^{T2} system, NSPCs were differentiated for 7 days, exposed to OH-TAM for 4 days, and then analyzed for neuronal differentiation. Strikingly, treatment of differentiated cells with OH-TAM led to a robust increase in MAP2AB-expressing neurons (Figures 3A and 3B). These findings indicate that ER^{T2}-based control of proneural gene expression is effective for driving neuronal differentiation in nondividing (i.e., ethynyl-deoxy-uridine [EdU] negative), differentiated astroglial cells (Figures 3A–3C).

After showing that fusion of TFs to an ER^{T2} motif is suitable for controlling gene expression in vitro, we next tested the system in vivo within the neurogenic niche of the adult hippocampus. We previously showed that retrovirus-mediated ASCL1 overexpression within the adult DG redirects the progeny of NSPCs away from a neuronal fate and toward the oligodendrocytic lineage (Jessberger et al., 2008). Therefore, NSPCs respond differently to ASCL1 overexpression in vivo (i.e., oligodendrocytic differentiation) and in vitro (i.e., neuronal differentiation). At this time, it remains unclear whether this is due to intrinsic differences or niche-derived cues that are responsible for the context-dependent behavior of adult hippocampal NSPCs (Jessberger et al., 2008). Be that as it may, we made use of this robust cellular phenotype and tested whether the system of retrovirus-mediated, TAM-controlled gene expression also functions in vivo. Animals were injected with *Ascl1*-ER^{T2}-expressing retroviruses and treated for 5 consecutive days with i.p. TAM injections (to switch the transgene on). Notably, 3 weeks after viral injection, the vast majority of newborn cells in the TAM-treated mice displayed an oligodendrocytic phenotype and expressed OLIG2, NG2, and SOX10 (Figures 4B–4D). These results phenocopied previous results obtained using noninducible retroviruses with constitutively active chicken beta-actin promoter driving *Ascl1*, although the phenotypic switch was not as complete (*Ascl1*-ER^{T2}: +TAM 73.96% ± 6.72% oligodendrocytes, constitutively active *Ascl1* overexpression: 87.52% ± 2.08% oligodendrocytes, resulting in an efficiency of 84.50% to redirect newborn cells toward the oligodendrocytic lineage using the ER^{T2}-based approach compared with constitutively active *Ascl1* overexpression; see also Jessberger et al., 2008). These data clearly indicate the functional induction of ASCL1 target gene expression using the *Ascl1*-ER^{T2} system within the adult hippocampus. In striking contrast, we observed almost no fate change of newborn cells toward the oligodendrocytic lineage in mice that were injected with *Ascl1*-ER^{T2}-expressing retroviruses but had not received TAM injections (Figures 4A and 4C). Notably, delayed onset of TAM administration, starting 4 weeks after stereotactic injections of *Ascl1*-ER^{T2}-expressing viruses, did not affect the fate-choice decisions of newborn cells in the adult DG, in contrast to the in vitro situation where glial cells could be redirected toward a neuronal fate upon TAM-induced ASCL1-ER^{T2} activation (Figures 3A–3C and S4B–S4E). In summary, these data further underline the tightness of the ER^{T2}-based system to drive gene expression in newborn cells.

DISCUSSION

We have described an approach that achieves inducible, retrovirus-mediated gene expression by using the coding sequence of TFs fused to an ER^{T2} motif. Fusion of the ER^{T2} motif to two TFs that regulate fate-choice decisions in the course of adult neurogenesis (i.e., ASCL1 and NEUROD1) allowed tight temporal control of functional gene expression in cultured NSPCs as well as within a neurogenic niche of the adult brain.

The approach described here extends the range of applications for retrovirus-mediated gene manipulation. This highly selective and extremely fast strategy to test gene function in the context of mammalian neurogenesis can be combined with an ER^{T2}-mediated system for temporal control of gene expression, allowing one to switch gene expression on (and off) with the use of TAM. Thus, with this simple two-step cloning protocol, it is now possible

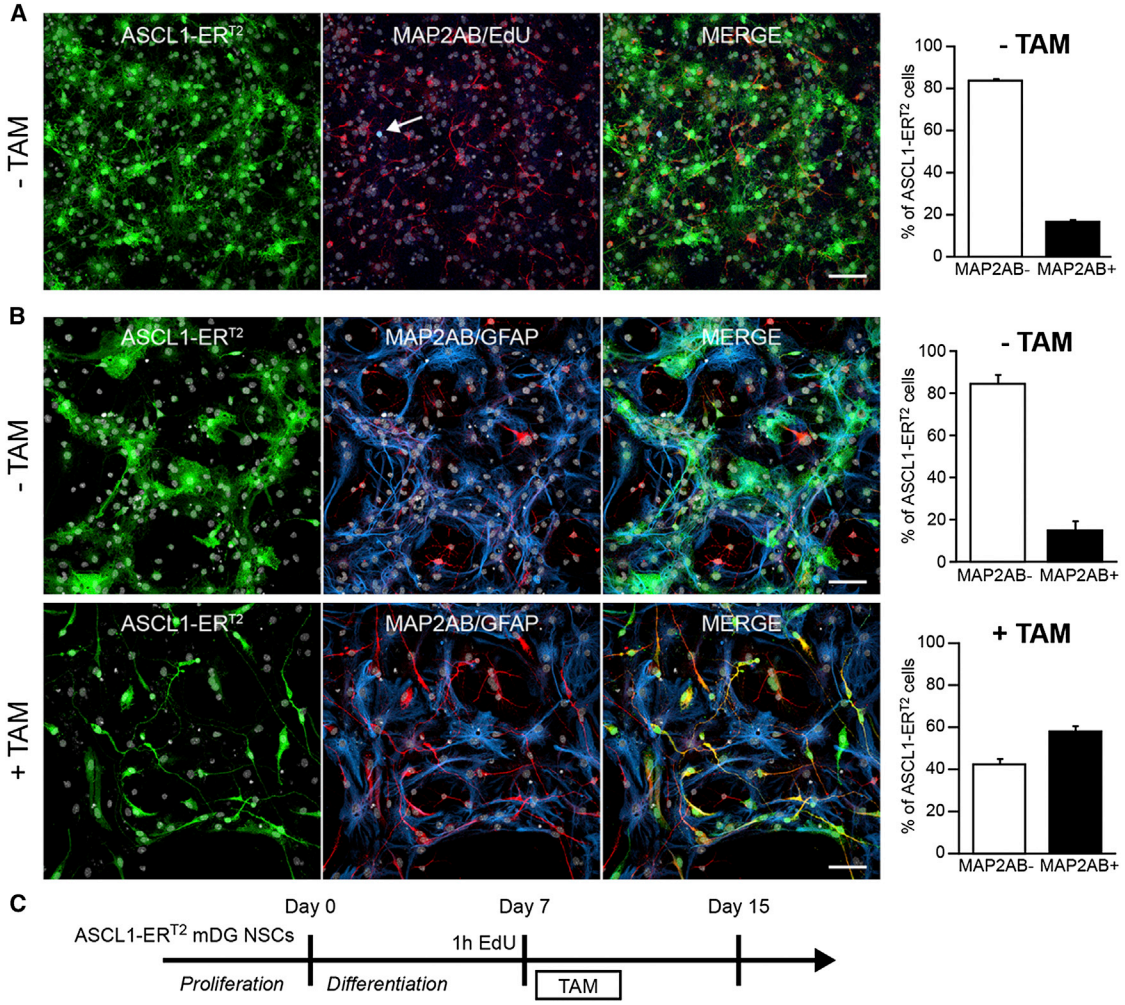

Figure 3. TAM Treatment Converts Astroglia toward a Neuronal Fate in Differentiated *Ascl1*-ER^{T2}-Expressing NSPCs

(A) *Ascl1*-ER^{T2}-expressing cells were differentiated for 7 days in the absence of OH-TAM and mainly gave rise to MAP2AB-negative differentiated astroglia. Right bars show quantifications. Notably, virtually all of the NSPCs (>99.5%) are negative for EdU (blue), indicating that the cells have exited the cell cycle and become postmitotic. The arrow points toward one of the rare EdU-labeled cells (n = 3, biological replicates).

(B) The vast majority of *Ascl1*-ER^{T2}-expressing cells (green) continue to differentiate into glial cells expressing GFAP (blue) and are negative for MAP2AB (red) in the absence of OH-TAM. In striking contrast, OH-TAM exposure 7 days after initiation of differentiation results in a robust increase in MAP2AB-expressing, neuronally differentiated cells, suggesting that OH-TAM-induced ASCL1 activity is also sufficient to drive neuronal differentiation in NSPC-derived cells that have adopted an astroglial fate. Right bars show quantifications. −TAM: 15.24% ± 4.84% neurons; +TAM: 57.80% ± 3.07% neurons; *p < 0.001; n = 3, biological replicates.

(C) Experimental design of delayed OH-TAM treatment.

Error bars represent mean ± SEM. Scale bars represent 40 μm. Nuclei were stained with DAPI (gray).

See also Figure S3.

to test the function of genes in distinct stages or for different durations during neural development both in vitro and in vivo.

Using this inducible system, we were able to dramatically increase the neuronal differentiation of NSPCs, with >90% of NSPC-derived cells differentiating into neurons in vitro, which is similar to the rate of neuronal differentiation observed within the hippocampal niche. Thus, the approach described here overcomes the problems associated with mixed neuronal and glial cultures. For example, proteomics or metabolomics studies comparing NSPCs with their neuronally differentiated progeny, which require large amounts of cells, can now be performed with reproducible

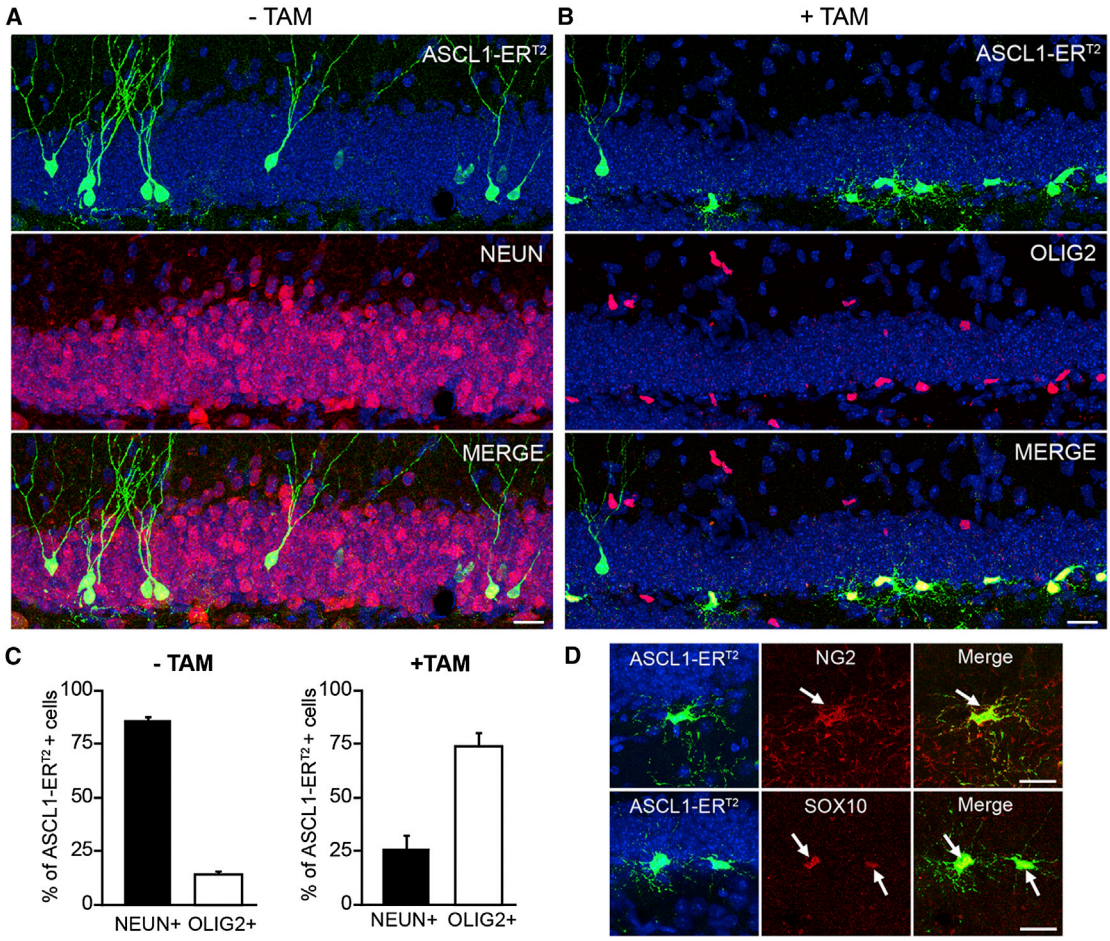

Figure 4. Inducible and Controllable Gene Expression in Newborn Cells within the Adult Hippocampus

(A) Injection of *Ascl1*-ER^{T2}-expressing retroviruses (green) into the adult DG without TAM treatment leads to the labeling of newborn granule cells (NEUN positive, red) 3 weeks after viral injection, similar to transduction of dividing cells with a control virus (data not shown), indicating that ASCL1 expression is not active without TAM-induced nuclear translocation.

(B) TAM treatment for 5 days after injection of *Ascl1*-ER^{T2}-expressing retroviruses induces oligodendrocytic differentiation (OLIG2 positive, red) of transduced cells within the adult DG, indicating the tight temporal control of gene expression in adult-born cells.

(C) Quantifications of the phenotypic shift induced by TAM-mediated activation of ASCL1 transcriptional activation in *Ascl1*-ER^{T2}-expressing cells. −TAM: 13.98% ± 1.92% oligodendrocytes; +TAM: 73.96% ± 6.72% oligodendrocytes; *$p < 0.001$; $n = 4$, biological replicates.

(D) TAM-induced gene expression in *Ascl1*-ER^{T2}-transduced cells (green) results in expression of NG2 (red, upper panels) and SOX10 (red, lower panels), indicating a fate switch from the neuronal toward the oligodendrocytic lineage.

Error bars represent mean ± SEM. Scale bar represents 20 μm. Nuclei were stained with DAPI (blue).

See also Figure S4.

and almost pure neuronal populations. We were also able to use inducible ASCL1 overexpression to convert NSPC-derived astrocytes into neurons. Furthermore, there is increasing evidence that newborn neurons of different ages have specific functions within the hippocampus; therefore, the newly developed inducible strategy may help improve our understanding of the molecular mechanisms that regulate distinct steps of newborn neuron maturation.

Clearly, the approach described here is not limited to studying genes in the context of adult neurogenesis. A large number of experiments aiming to manipulate TFs will benefit from an ER^{T2}-based temporal control of gene expression (in retroviral or plasmid DNA format) in both adult and embryonic tissues (e.g., using in utero electroporation of plasmids encoding for TF-ER^{T2}-fusion proteins). In addition, the approach described here will be useful for studying the temporal requirements of selected TFs in the

context of cellular reprogramming of somatic cells toward distinct lineages or pluripotency (Takahashi and Yamanaka, 2006; Vierbuchen et al., 2010).

EXPERIMENTAL PROCEDURES

Cloning

The complementary DNA (cDNA) sequence of *Ascl1* and *NeuroD1* TFs was fused to the ER^{T2} motif by fusion PCR as described in Figure 1A and Supplemental Experimental Procedures. TF and ER^{T2} cDNA fragments were PCR amplified individually (PCR 1: primers P1 and P2, TF cDNA as template; PCR 2: primers P3 and P4, ER^{T2} cDNA as template). The PCR products were then used as templates for the fusion PCR reaction (PCR 3: primers P1 and P4, products of PCR 1 and 2 as template).

Note: Phusion polymerase (NEB) was used for the PCR reactions (cycling parameters: 98°C 30 s, 60°C 45 s, 72°C 1 min [30 cycles]). Primers P2 and P3 were designed so that 20 bases would be complementary to each other. To improve PCR amplification, all primers should be designed within a similar T_m range (see Supplemental Experimental Procedures for information regarding primer design).

The fusion PCR product, TF-ER^{T2}, was then cloned into a replication-incompetent Moloney murine leukemia virus construct, pCAG-IRES-GFP (mCherry or CFP). The vector was digested with BamHI restriction enzymes (NEB), blunted with Klenow polymerase (NEB), dephosphorylated with alkaline-phosphatase (Roche), and ligated with the fusion PCR product using T4 DNA ligase (Roche). Positive clones were evaluated by NheI restriction digest and their sequence was confirmed by DNA sequencing. The product of these reactions was the retroviral vector pCAG-TF-ER^{T2}-IRES-GFP (mCherry or CFP).

Virus Production

Viruses were produced as previously described (Zhao et al., 2006). In brief, ten 10 cm plates of confluent human embryonic kidney (HEK293T) cells were transfected with retroviral constructs and packaging plasmids (pCMV-vsvg and pCMV-gp) using Lipofectamine 2000 (Invitrogen). Two days after transfection, the virus containing cell culture media (100 mL) was collected, filtered with a 0.22 μm Steritop filter (Millipore), and centrifuged at 19,400 rpm in an ultracentrifuge for 2 hr at 4°C. The viral pellet was resuspended in 4 ml PBS and centrifuged a second time through a 20% sucrose cushion at 19,400 rpm for 2 hr at 4°C. The final viral pellet was resuspended in 40 μl of PBS and used for subsequent infections.

Cell Culture

Wild-type mouse DG NSPCs (WT mDG NSPCs) were isolated as previously described (Bracko et al., 2012). The resulting single-cell suspension was cultured as a sphere culture in Dulbecco's modified Eagle's medium (DMEM)/F12 medium supplemented with B27 (Invitrogen), human epidermal growth factor (20 ng/ml), and human basic fibroblast growth factor 2 (20 ng/ml; Peprotech). The medium contained an antibiotic/antimycotic (Anti-Anti; Invitrogen). Cells were then plated on glass coverslips coated with poly-L-ornithine (Sigma) and laminin (Invitrogen), and heparin (5 μg/mL) was added to the medium to obtain adherent cultures. All experiments were done in triplicates. To analyze the efficacy of the TF-ER^{T2} system in vitro, WT mDG NSPCs were infected with *Ascl1*-ER^{T2}-IRES-GFP retrovirus, *NeuroD1*-ER^{T2}-IRES-GFP retrovirus, or CAG-IRES-GFP retrovirus as a control. They were expanded for 24 hr for acute experiments and passaged for several weeks for passaged cell experiments. Differentiation was induced by growth factor withdrawal in the presence and absence of hydroxy-TAM (OH-TAM; 0.5 μM). OH-TAM was present in the differentiating medium for 2 days or a maximum of 4 days. The medium was changed every 2–3 days. Cells were fixed 7 days after the onset of differentiation or exposed to OH-TAM for 4 days and further differentiated for an additional 4 days. NSPC proliferation was measured using a 1 hr pulse with EdU (10 μM; Sigma) at 37°C followed by paraformaldehyde (PFA) fixation. EdU stainings were performed before antibody incubation using the Click-iT EdU Imaging Kit (Invitrogen) according to the manufacturer's protocol.

Animals

All animal experiments were approved by the veterinary office of the Canton of Zurich, Switzerland. Mice were kept with littermates under a 12 hr dark/light cycle in single ventilated cages and with ad libitum access to food and water. Virus injections were performed as previously described (Knobloch et al., 2013). To test *Ascl1*-ER^{T2}-expressing retroviruses in vivo, 6- to 8-week-old WT mice were stereotactically injected in the DG with 1.5 μl *Ascl1*-ER^{T2}-IRES-GFP-expressing retroviruses (Karalay et al., 2011). In the first set of experiments, the day after retrovirus injection, animals received the first of five consecutive daily i.p. injections of TAM dissolved in sunflower oil (100 mg/kg, both reagents from Sigma). As a control, animals injected with the retroviruses did not receive TAM injections. The animals were killed 3 weeks after the last TAM injection (n = 4 for each condition). In the second set of experiments, mice were injected with *Ascl1*-ER^{T2}-IRES-GFP-expressing retroviruses and red fluorescent protein (RFP)-expressing retroviruses (Vadodaria et al., 2013) as a control. These mice received 5 daily TAM injections 4 weeks after viral injections and were killed 1 week after the last TAM injection (n = 4). To test for directed differentiation efficiency of the ER^{T2}-based approached compared with constitutive ASCL1 overexpression, we injected *Ascl1*-IRES-GFP-expressing retroviruses into WT mice and killed the animals 3 weeks later (n = 4).

For tissue collection, mice were given a lethal dose of Esconarkon (Streuli) and flushed transcardially with 0.9% sterile NaCl, followed by fixation with 4% PFA/0.1 M phosphate buffer, pH 7.4. The brains were postfixed in 4% PFA/0.1 M phosphate buffer overnight at 4°C, followed by 30% sucrose/0.1 M phosphate buffer, and stored at 4°C.

Immunohistochemistry

We cut the brains into 40-μm-thick free-floating sections by snap-freezing them with dry ice after mounting them on a microtome as described previously (Karalay et al., 2011). For blocking, we used 1× TBS containing 3% donkey serum and 0.25% Triton X-100 for 30 min. Primary antibody incubation was done overnight at

4°C in the concentrations specified below. Secondary antibodies (Jackson ImmunoResearch) were applied at 1:250 at room temperature for 1 hr. Cell nuclei were counterstained with DAPI (1:5,000; Sigma). For cell stainings, immunocytochemistry was performed as described above on cells fixed with 4% PFA for 15 min at 37°C. The antibodies used were chicken α-GFP (1:500; Aves), mouse α-MAP2AB (1:500; Sigma), rabbit α-GFAP (1:500; Dako), goat α-SOX2 (1:250; Santa Cruz), mouse α-NEUN (1:200; Millipore), rabbit α-OLIG2 (1:250; Millipore), rabbit α-NG2 (1:500; Millipore), goat α-SOX10 (1:100; Santa Cruz), goat α-NEUROD1 (1:250; Santa Cruz), and rabbit α-DsRed/RFP (Clontech; 1:500).

Luciferase Assays

We electroporated *Ascl1*-ERT2-expressing NSPCs with pE3x6 Luciferase (Castro et al., 2006) and pTk Renilla constructs using a nucleofector device (Amaxa). The NSPCs were then treated with OH-TAM for 0, 5, 10, and 24 hr. The cells were then lysed in PLB lysis buffer (Promega). We determined Luciferase and Renilla activity using the Dual Luciferase reporter assay (Promega). Luminescence was measured with a Novostar plate reader. Transcriptional activity was determined as the ratio of Luciferase activity over Renilla activity.

Image Analysis

For colocalization experiments and cell quantifications, we performed confocal microscopy (AOBS-SP2; Leica) followed by colocalization analyses using ImageJ with the Cell Counter plugin. Photoshop (CS5) was used for contrast enhancements and color adjustments.

Western Blot

HEK293T cells were transfected with retroviral constructs expressing *Ascl1*, *Ascl1*-ER^{T2}, *NeuroD1*, or *NeuroD1*-ER^{T2} using Lipofectamine (Invitrogen). Cells were lysed and extracted protein concentrations were determined by Bradford assay (BioRad). Proteins were separated by SDS-PAGE electrophoresis, transferred to a nitrocellulose membrane (BioRad), and probed with primary antibodies, goat α-NEUROD1 (1:1,000; Santa Cruz), mouse α-ASCL1 (1:1,000; BD), mouse α-GAPDH (1:10,000; HyTest), and rabbit α-MATRIN3 (1:2,000; Bethyl) followed by horseradish-peroxidase-conjugated secondary antibodies (Jackson ImmunoResearch), and bands were detected by chemiluminescence (Thermo Scientific).

Fractionation of Cytoplasmic and Nuclear Proteins

Fractionations were performed as previously described (Knobloch et al., 2013). *Ascl1*-ERT2-expressing NSPCs were lysed in 0.5% Triton buffer. Lysates were centrifuged at 13 krpm for 15 min at 4°C to separate insoluble nuclei. The supernatant containing the membrane proteins was removed and stored on ice. The nuclear pellet was rinsed twice with lysis buffer and then resuspended in lysis buffer containing 0.5% SDS and sonicated. The samples were precleared by centrifugation at 13 krpm for 15 min at 4°C and the supernatant containing the nuclear proteins was stored on ice. The samples were then used for western blot analysis.

Statistical Analyses

Statistical analyses were performed using Excel (Microsoft). Two sample t tests were used for all comparisons. Differences were considered significant at $p < 0.001$.

SUPPLEMENTAL INFORMATION

Supplemental Information includes four figures and Supplemental Experimental Procedures and can be found with this article online at http://dx.doi.org/10.1016/j.stemcr.2013.06.003.

ACKNOWLEDGMENTS

We thank Burkhard Becher for conceptual input, Fred H. Gage for critical comments on the manuscript, François Guillemot for bHLH luciferase constructs, and the Center for Microscopy and Image Analysis (ZMB) of the University of Zurich and the Light Microscopy and Screening Center (LMSC) of ETH Zurich for help with imaging. This work was supported by the NCCR Neural Plasticity and Repair, Swiss National Science Foundation, Zurich Neuroscience Center (ZNZ), and the EMBO Young Investigator Program (to S.J.).

Received: January 24, 2013
Revised: June 4, 2013
Accepted: June 5, 2013
Published: July 11, 2013

REFERENCES

Babu, H., Cheung, G., Kettenmann, H., Palmer, T.D., and Kempermann, G. (2007). Enriched monolayer precursor cell cultures from micro-dissected adult mouse dentate gyrus yield functional granule cell-like neurons. PLoS ONE *2*, e388.

Bracko, O., Singer, T., Aigner, S., Knobloch, M., Winner, B., Ray, J., Clemenson, G.D., Jr., Suh, H., Couillard-Despres, S., Aigner, L., et al. (2012). Gene expression profiling of neural stem cells and their neuronal progeny reveals IGF2 as a regulator of adult hippocampal neurogenesis. J. Neurosci. *32*, 3376–3387.

Castro, D.S., Skowronska-Krawczyk, D., Armant, O., Donaldson, I.J., Parras, C., Hunt, C., Critchley, J.A., Nguyen, L., Gossler, A., Gottgens, B., et al. (2006). Proneural bHLH and Brn proteins coregulate a neurogenic program through cooperative binding to a conserved DNA motif. Dev. Cell. *11*, 831–844.

Dhaliwal, J., and Lagace, D.C. (2011). Visualization and genetic manipulation of adult neurogenesis using transgenic mice. Eur. J. Neurosci. *33*, 1025–1036.

Gao, Z., Ure, K., Ables, J.L., Lagace, D.C., Nave, K.A., Goebbels, S., Eisch, A.J., and Hsieh, J. (2009). Neurod1 is essential for the survival and maturation of adult-born neurons. Nat. Neurosci. *12*, 1090–1092.

Ge, S., Goh, E.L., Sailor, K.A., Kitabatake, Y., Ming, G.L., and Song, H. (2006). GABA regulates synaptic integration of newly generated neurons in the adult brain. Nature *439*, 589–593.

Heinrich, C., Blum, R., Gascon, S., Masserdotti, G., Tripathi, P., Sanchez, R., Tiedt, S., Schroeder, T., Gotz, M., and Berninger, B.

(2010). Directing astroglia from the cerebral cortex into subtype specific functional neurons. PLoS Biol. *8*, e1000373.

Ihrie, R.A., Shah, J.K., Harwell, C.C., Levine, J.H., Guinto, C.D., Lezameta, M., Kriegstein, A.R., and Alvarez-Buylla, A. (2011). Persistent sonic hedgehog signaling in adult brain determines neural stem cell positional identity. Neuron *71*, 250–262.

Indra, A.K., Warot, X., Brocard, J., Bornert, J.M., Xiao, J.H., Chambon, P., and Metzger, D. (1999). Temporally-controlled site-specific mutagenesis in the basal layer of the epidermis: comparison of the recombinase activity of the tamoxifen-inducible Cre-ER(T) and Cre-ER(T2) recombinases. Nucleic Acids Res. *27*, 4324–4327.

Iwano, T., Masuda, A., Kiyonari, H., Enomoto, H., and Matsuzaki, F. (2012). Prox1 postmitotically defines dentate gyrus cells by specifying granule cell identity over CA3 pyramidal cell fate in the hippocampus. Development *139*, 3051–3062.

Jessberger, S., Toni, N., Clemenson, G.D., Jr., Ray, J., and Gage, F.H. (2008). Directed differentiation of hippocampal stem/progenitor cells in the adult brain. Nat. Neurosci. *11*, 888–893.

Jiang, J., Yu, H., Shou, Y., Neale, G., Zhou, S., Lu, T., and Sorrentino, B.P. (2010). Hemgn is a direct transcriptional target of HOXB4 and induces expansion of murine myeloid progenitor cells. Blood *116*, 711–719.

Karalay, O., Doberauer, K., Vadodaria, K.C., Knobloch, M., Berti, L., Miquelajauregui, A., Schwark, M., Jagasia, R., Taketo, M.M., Tarabykin, V., et al. (2011). Prospero-related homeobox 1 gene (Prox1) is regulated by canonical Wnt signaling and has a stage-specific role in adult hippocampal neurogenesis. Proc. Natl. Acad. Sci. USA *108*, 5807–5812.

Knobloch, M., Braun, S.M., Zurkirchen, L., von Schoultz, C., Zamboni, N., Araúzo-Bravo, M.J., Kovacs, W.J., Karalay, O., Suter, U., Machado, R.A., et al. (2013). Metabolic control of adult neural stem cell activity by Fasn-dependent lipogenesis. Nature *493*, 226–230.

Sahay, A., Scobie, K.N., Hill, A.S., O'Carroll, C.M., Kheirbek, M.A., Burghardt, N.S., Fenton, A.A., Dranovsky, A., and Hen, R. (2011). Increasing adult hippocampal neurogenesis is sufficient to improve pattern separation. Nature *472*, 466–470.

Seaberg, R.M., Smukler, S.R., and van der Kooy, D. (2005). Intrinsic differences distinguish transiently neurogenic progenitors from neural stem cells in the early postnatal brain. Dev. Biol. *278*, 71–85.

Takahashi, K., and Yamanaka, S. (2006). Induction of pluripotent stem cells from mouse embryonic and adult fibroblast cultures by defined factors. Cell *126*, 663–676.

Vadodaria, K.C., Brakebusch, C., Suter, U., and Jessberger, S. (2013). Stage-specific functions of the small rho GTPases cdc42 and rac1 for adult hippocampal neurogenesis. J. Neurosci. *33*, 1179–1189.

van Praag, H., Schinder, A.F., Christie, B.R., Toni, N., Palmer, T.D., and Gage, F.H. (2002). Functional neurogenesis in the adult hippocampus. Nature *415*, 1030–1034.

Vierbuchen, T., Ostermeier, A., Pang, Z.P., Kokubu, Y., Südhof, T.C., and Wernig, M. (2010). Direct conversion of fibroblasts to functional neurons by defined factors. Nature *463*, 1035–1041.

Zhao, C., and Gage, F.H. (2008). Retrovirus-mediated cell labeling. In Adult Neurogenesis, F.H. Gage, ed. (Long Island, NY: CSHL Press), pp. 111–117.

Zhao, C., Teng, E.M., Summers, R.G., Jr., Ming, G.L., and Gage, F.H. (2006). Distinct morphological stages of dentate granule neuron maturation in the adult mouse hippocampus. J. Neurosci. *26*, 3–11.

Zhao, C., Deng, W., and Gage, F.H. (2008). Mechanisms and functional implications of adult neurogenesis. Cell *132*, 645–660.